ARCHIVIO ISTITUZIONALE
DELLA RICERCA

Alma Mater Studiorum Università di Bologna
Archivio istituzionale della ricerca

Fluorinated Biphenyl Phosphine Ligands for Accelerated [Au(I)]-Catalysis

This is the final peer-reviewed author's accepted manuscript (postprint) of the following publication:

Published Version:
Pedrazzani, R., Kiriakidi, S., Monari, M., Lazzarini, I., Bertuzzi, G., Silva López, C., et al. (2024). Fluorinated Biphenyl Phosphine Ligands for Accelerated [Au(I)]-Catalysis. ACS CATALYSIS, 14, 6128-6136 [10.1021/acscatal.4c00593].

Availability:
This version is available at: https://hdl.handle.net/11585/1001854 since: 2025-01-16

Published:
DOI: http://doi.org/10.1021/acscatal.4c00593

Terms of use:

Some rights reserved. The terms and conditions for the reuse of this version of the manuscript are specified in the publishing policy. For all terms of use and more information see the publisher's website.

This item was downloaded from IRIS Università di Bologna (https://cris.unibo.it/).
When citing, please refer to the published version.

(Article begins on next page)

24 May 2025

Fluorinated Biphenyl Phosphine Ligands for Accelerated [Au(I)]-Catalysis

Riccardo Pedrazzani,[a] Sofia Kiriakidi,[b] Magda Monari,*[a,c] Irene Lazzarini,[a] Giulio Bertuzzi,[a,c] Carlos Silva López,*[b] Marco Bandini*[a,c]

[a] Dipartimento di Chimica "Giacomo Ciamician", Alma Mater Studiorum – Università di Bologna, via Selmi 2, 40126, Bologna – Italy. [b] Departamento de Química Orgánica, Universidade de Vigo, AS Lagoas (Marcosende) s/n, 36310 Vigo, Spain. [c] Center for Chemical Catalysis - C3, via Selmi 2, 40126, Bologna – Italy.

KEYWORDS. [Au(I)] catalysis, Computational analysis, Fluorinated compounds, Phosphine ligands, Alkynes.

ABSTRACT: Fluorinated JohnPhos-type ligands are proposed as accelerating tools in homogenous gold(I) catalysis with *PedroPhosAu*Cl (**Cat 1**) as the most efficient one. The ligands as well as the corresponding gold complexes were synthetized in high yields and fully characterized also via single-crystal X-ray spectroscopy. A secondary interaction between the distal phenyl ring of the phosphane ligand and the metal center is identified as key for the fine-tuning of the overall catalytic performance of the complexes. In particular, kinetic as well as computational analysis revealed that by accommodating F atoms on the biphenyl pendant of the ligand, more reactive organo-gold intermediates are realized toward subsequent nucleophilic condensations. The gold catalyzed indole-hydroarylation of 1,6-enynes and the intramolecular hydroindolynation of alkynes have been adopted as benchmark reactions to exemplify these accelerating effects.

Homogenous gold catalysis has reached an extraordinary level of maturity, robustness, and predictability in terms of chemical and stereochemical outcomes with a special focus on site-selective manipulations of unsaturated hydrocarbons.[1] The success of gold catalysis in covering a broad range of chemical spaces and is largely attributable to the substantial efforts devoted to the design of organic ligands.[2] A high level of complexity is nowadays available in this context, enabling gold catalysis to penetrate challenging areas of modern organic synthetic chemistry.[3]

The *remote* steric, as well as electronic perturbation of organic ligands, has been extensively explored in homogenous gold catalysis, reaching a remarkable level of fine-tuning for the corresponding metal species.[4] Among many, P-based ligands have played a pivotal role, utilizing bulky dialkylbiarylphosphanes (Buchwald phosphanes)[5] as elective scaffolds for [Au(I)]-promoted transformations.[6] In this context, Echavarren achieved a landmark developing a family of easy-to-handle silver-free cationic [Au(I)] complexes that significantly contributed to the field.[7] The outstanding catalytic performance of the commercially available [JohnPhosAu(ACN)]SbF_6] relies on an interplay of multiple steric as well as electronic features of the phosphane. In particular, the *ortho*-biphenyl group is responsible for stabilizating interactions with the metal center during the catalytic cycle via tailored η^1/η^2 coordination modes. Interestingly, ligands comprising this architecture commonly feature electron-donating substituents at the outer phenyl ring (*i.e.* *i*PrO, *i*Pr, NR_2), thus enhancing a stabilizing donor effect of the biphenyl pendant onto the electrophilic gold center (Figure 1a). Additionally, the presence of a bulky alkyl group at the P center would prevent free-rotations about the C_2-P connection, with a consequent beneficial impact on the conformational stability of the resulting Au complex.

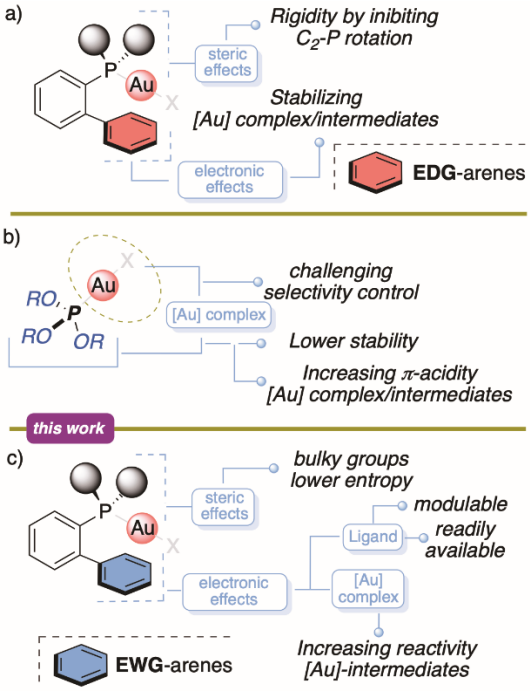

Figure 1. a) Classic dialkylbiarylphosphane ligands featuring stabilizing groups at the outer phenyl ring and rotational constrains at the coordinating site (P). b) Phosphite-like ligands are utilized to generate highly electrophilic gold complexes. c) The proposed new class of EWG-containing phosphane ligands that merged both a) and b) approaches.

An alternative strategy to tackle catalytic activity in gold catalysis relies on increasing the π-acidity of the metal center by introducing strong electron-withdrawing units at the phosphorus atom (*i.e.* alkoxy, aryloxy and nitrogen containing groups, Figure 1b). The use of phosphite-like and phosphonite-like ligands[8] although frequently successful, results in more moisture-sensitive and less functional group tolerant gold complexes. In addition, the presence of an open catalytic site (dashed area) can lead to selectivity issues due to an unconstrained catalytic environment.

To address these challenges, the proposed approach involves combining the robustness of alkyl/aryl phosphines with the higher electrophilicity imprinted by EWG-comprising ligands, we speculated that the introduction of fluorinated groups/atoms at the outer unit of the biphenyl moiety could integrate and merge both aspects in a single platform that has never been explored systematically in homogeneous gold catalysis (Figure 1c).[4b,9] The rationale behind this approach is to design a catalytic system that benefits from both the stability and functional group tolerance of alkyl/aryl phosphines and the increased electrophilicity brought about by the introduction of fluorinated groups. By doing so, the aim is to optimize catalytic performance and overcome the limitations associated with previous strategies, ultimately providing a more efficient and selective homogeneous gold catalysis platform.

At the beginning of our investigation, we drew inspiration from our recent results involving CF_3-containing imidazo[1,5-a]pyridin-3-ylidene platforms (ImPys) for gold catalyzed activation of allenes and alkynes.[10] Building upon this, our focus shifted towards incorporating fluorine atoms and CF3 groups onto the outer phenyl ring of the biphenyl core of JohnPhos-inspired (**A1**,**2**). Here, the Suzuki-Miyaura cross coupling between *ortho*-bromo iodobenzene and the desired fluorinated aryl-boronic acids (see supporting information for details) proved to be highly efficient to access fluorinated *ortho*-bromo biphenyls in high isolated yields (84%). Additionally, the dimethoxy-based biaryl **A3** was successfully synthesized using a similar approach, yielding 89%. This compound serves as a benchmark to assess the impact of fluorinated rings more accurately on the resulting gold complexes.

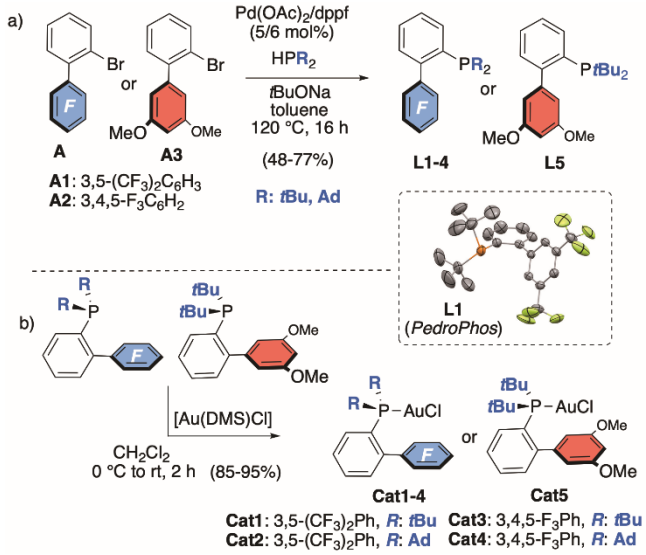

Scheme 1. a) Synthesis of biaryl-based phosphines **L1-5** via Pd-catalyzed phosphination of bromoarenes. b) Synthesis of the phosphino gold(I) chloride complexes (**Cat1-5**) studied in the present investigation.

Phosphination of the bromoarenes **A1-3** was then conveniently performed via Pd-mediated cross-coupling reactions ($Pd(OAc)_2$, dppf)[4b] in the presence of secondary phosphines (HPR_2, R = *t*Bu, Ad) as nucleophiles.[11] Satisfyingly, the corresponding bulky phosphanes **L1-5** were isolated as white solids in moderate to high yields (48-77%, Scheme 1 top, **L1**: cited hereafter as *PedroPhos*).

Consequently, the targeted gold chloride complexes, denoted as **Cat1-5** (with **Cat1** referred to as *PedroPhosAuCl* henceforth) were successfully obtained. These complexes exist as air stable white solids and were obtained in nearly quantitative yields (85-95%) via complexation of ligands **L1-5** with [Au(DMS)Cl] under mild conditions.

Structural analysis of **Cat1-5** at the solid state was carried out via single crystal X-ray diffraction (SC-XRD), and a collection of structural parameters are reported in Table 1. As expected, all crystals obtained showed the common P-Au-Cl linear architecture, lying almost parallel to the outer arene (Au-P-C-C dihedral angles = 0-11.0°, where C-C is the bond connecting the two aromatic rings). The resulting $Ar_F\cdots Au$ interactions turned out to be stronger, with consequent shorter $Ar_F\cdots Au$ contacts (**Cat1** and **Cat3**, entries 1 and 2)[12] in comparison to electron neutral structural analogous JohnPhosAuCl (entry 3).

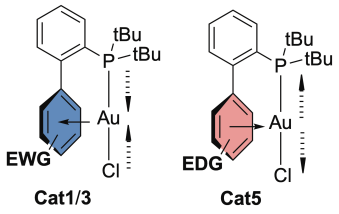

Chart 1.

This metal/arene orbital interaction resulted in a shortened Au-P and Au-Cl bonds, suggesting an electron density migration from metal to ligand as predominant in the $Ar_F\cdots Au$ contact. Interestingly, placing an electron rich aryl unit at the biphenyl core of the ligand (**L5**) caused an almost identical Ar···Au distance (3.267 Å) to the electron poor ones (entry 4 *vs* entries 1-2). However, the elongation of both the corresponding Au-P bond (2.254 Å) and Au-Cl bond (2.304 Å) can be referred to a ligand-to-metal electron density migration as the most relevant in **Cat5** (Chart 1).

Table 1. Solid-state analysis of Cat1-5 in comparison to JohnPhosAuCl and AdJohnPhosAuCl.

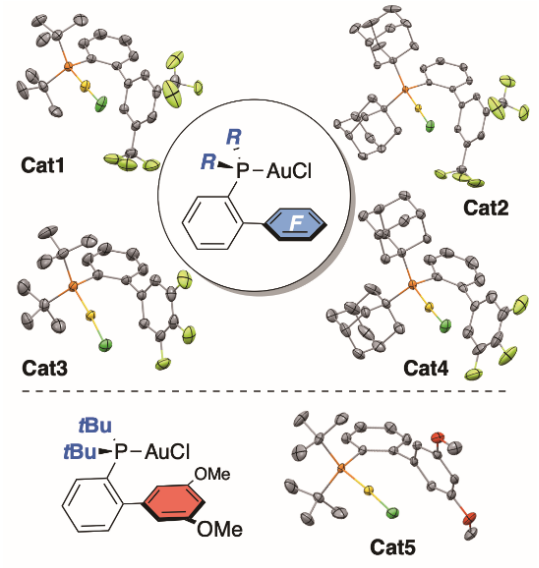

Entry	Cat	P-Au [Å]	Au-Cl [Å]	Ar…Au [Å][a]
1	*PedroPhosAuCl*	2.235 (1)	2.286 (1)	3.250
2	Cat3[b]	2.238 (1)	2.281 (1)	3.327
3	JohnPhosAuCl[c]	2.254 (3)	2.303 (4)	3.350
4	Cat5	2.267 (2)	2.304 (2)	3.267
5	Cat2	2.254 (1)	2.286 (1)	3.241
6	Cat4	2.257 (2)	2.293 (2)	3.213
7	AdJohnPhosAuCl[d]	2.254 (1)	2.301 (1)	3.337

[a] Distance between Au center and six-membered ring center of mass, calculated by Mercury. [b] Data reported for only one of the two independent molecules in the asymmetric unit. [c] Data obtained from CCDC 605716. [d] Data obtained from CCDC 1990417.

These structural solid state results were also reproduced via solution phase DFT calculations on the five catalysts using the long-range corrected functional ωB97XD,[13] and the 6-31+G(d,p) basis set, while the inner electrons of Au were described by the SDD effective core potential.[14] All calculations were performed with the Gaussian 16 code.[15] The computational results are in excellent agreement with the X-ray structures revealing a shorter distance between Ar and Au in case of both EWG **Cat1**/**3** and EDG **Cat5** compared to JohnPhosAuCl. However, while in the first cases shorter Au-P and Au-Cl distances were recorded, for **Cat5** both Au-P and Au-Cl bonds are elongated with respect to **JP** (Table S3), supporting a reverse electronic donating-accepting role for F-containing complexes and **Cat5** (Chart 1). Moreover, the P-Au-Cl bond lays parallel to the C-C bond connecting the two aromatic rings while the gold atom sits on top of the distal aromatic ring (see Scheme S3), in excellent agreement with the crystallography results. Non-covalent interactions (NCI) and topology analyses showed no critical bond points between the Au atom and the arene ring. Thus, there is no covalent bonding between the two moieties (for detailed results, see Scheme S4). Additionally, the inter-arene dihedral angle values for the computed and the X-ray structures of the catalysts were analyzed and found in good agreement (see Table S4).

The bis-adamantyl phosphine derivatives exhibited a similar trend in the gold complexes **Cat2** and **Cat4**. As a matter of fact, both species showed strongest Ar···Au π-interactions when compared to AdJohnPhosAuCl (entries 5-6 vs. entry 7) and a shortened Au-Cl bond. In this series, the Au-P bond is not significantly affected, likely due to the dominance of the bulky and electron rich bisadamantyl phosphine moiety.

To examine the catalytic performance of the synthetized gold(I) complexes and assess the impact of fluorine-decorated rings as pendants, the gold catalyzed hydroarylation of 1,6-enynes **1** was initially investigated.[12a,g,16] Our choice was dictated by the fact that both kinetic profile and chemoselectivity (*i.e.* carbocationic (**3a**) vs. carbenoic (**3a'**) pathway *vide infra*) have been frequently reported to reflect steric as well as electronic features of the gold catalyst. To this end, model enyne **1a** and indole **2** were reacted under mild conditions (CH_2Cl_2, rt) in the presence of a range of *in-situ* activated [Au(**L1-5**)Cl]/$AgSbF_6$ complexes (1 mol%). As a reference, commercially available [JohnPhosAu(ACN)]SbF_6 and [AdJohnPhosAuCl] (activated by $AgSbF_6$) catalysts were also tested under the same conditions, and the resulting outcomes are highlighted in Table 2. Reaction times as short as 1 h were considered to properly magnify the structure/activity relationship. From the data collected in Table 2, some preliminary considerations can be drawn.

Firstly, the presence of bulky adamantyl units at the P-center proved detrimental for the present transformation compared to the *t*Bu ones, regardless of the nature of the biphenyl substitution (*i.e.* 1 vs. 2 and 3 vs. 4). Focusing on the substitution of the distal phenyl ring, the 3,5-$(CF)_3$ pattern (**Cat1**, entry 1, yield = 95%, TOF: 330 h^{-1}, TON = 95)[17] conferred similar catalytic properties with respect to the 3,4,5-F_3 ones (**Cat3**, yield = 93%, entry 3) and both performed significantly better than [JohnPhosAu(ACN)]SbF_6 (entry 6, yield = 70%, TOF: 107 h^{-1}, TON = 70).[17] Interestingly, **Cat5**, comprising 3,5-$(OMe)_2$ substitution, promoted the cyclization reaction only in 48% yield (TOF: 85 h^{-1}, TON = 48),[17] supporting the accelerating effect promoted by EWG groups. It is also worth mentioning that preactivated cationic [**Cat1**-SbF_6] species performed similarly (entry 8, yield = 85%) to the *in situ* activated one and no erosion in the chemical outcome was observed by scaling the reaction to 1 mmol of **1a** (entry 9, yield = 89%).

Table 2. Monitoring the catalytic performance of Cat1-5 in comparison to [JohnPhosAu(ACN)]SbF_6 and [AdJohnPhosAuCl]/$AgSbF_6$

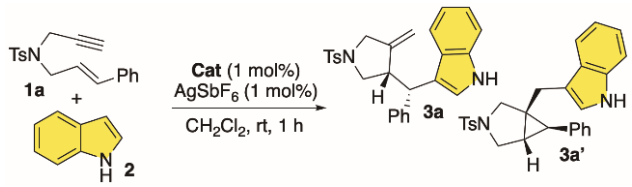

Run[a]	Cat	Yield **3a** (%)[b]	3a:3a'[c]
1	*PedroPhosAuCl*	95	> 25:1
2	Cat2	36[d]	ND
3	Cat3	93	24:1
4	Cat4	15[d]	ND

5	Cat5	48	> 25:1
6[e]	JohnPhosAuSbF$_6$	70	3.5:1
7	AdJohnPhosAuCl	NR	--
8[e]	[**Cat1**-SbF$_6$]	85	> 25:1
9[f]	Cat1	89	> 25:1

[a] All reactions were carried out under nitrogen atmosphere with dry solvents (**1a**: 0.2 mmol, **1a**/**2**: 1/1.2). [b] Isolated yield after flash chromatography as an average of three runs. [c] Determined on the reaction crude via ^{1}H-NMR analysis. [d] Large amounts of **1a** were recovered unreacted. [e] Silver-free conditions were applied. [f] Reaction on 1 mmol scale of **1a**. NR: no reaction. ND: not determined.

In parallel, the chemoselectivity of the procedure was significantly influenced by the features ligand. In this scenario, the presence of substituted outer phenyl rings on the ligand ensured high chemoselectivity towards the isomer **3a** (> 25:1), irrespective of their electronic properties. Contrarily, the use of an unsubstituted JohnPhos ligand resulted in poor chemical outcome yielding a mixture of **3a** and **3a'** with a ratio of 3.5:1 (entry 6).

In order to shed light onto the underlying mechanism and provide explanation for the chemo- and stereoselectivity of the studied reaction, we conducted DFT calculations using the simple JohnPhosAuCl and *PedroPhos*AuCl catalysts and the model enyne **1a**/indole **2** cyclization.[2b] The B3LYP[18]/6-31+G(d,p) level of theory was used for the reactivity investigation, while the inner electrons of Au were described by the SDD effective core potential. This is not the optimal DFT combination for gold catalysis but, considering the size and complexity of the structures at hand, it is a good cost-effective model according to *ad-hoc* benchmarks.[19]

The results obtained are summarized in Scheme 2 and show excellent agreement with the experimental data.

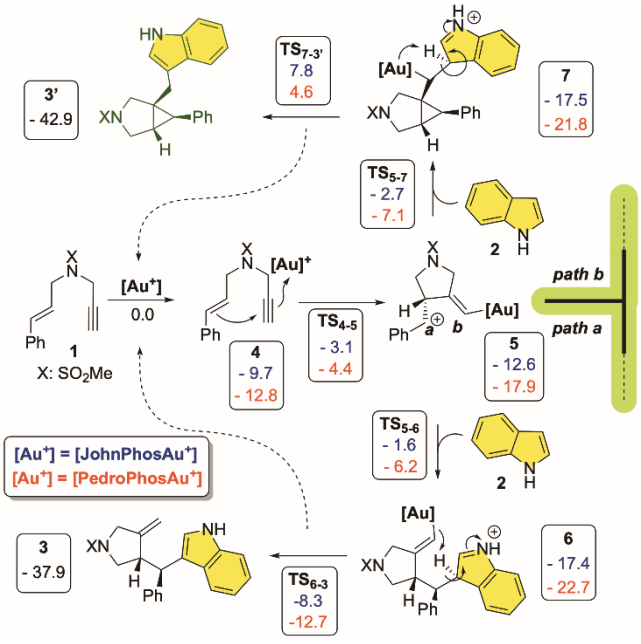

Scheme 2. Suggested reaction mechanism (enyne **1a** was simplified with *N*Ms analogous **1**). The energies correspond to minima (under each structure) and transition states (by the reaction arrows connecting two minima). Energies for the JohnPhosAu catalyst are depicted in blue whereas the ones for the *PedroPhos*Au in red.

The energy profile relative to the JohnPhos-based catalyst indicate that, initially, a precomplex (**4**) is formed between the cationic Au catalyst and the substrate (**1**) in a barrierless and exergonic manner (ΔG = -9.7 kcal/mol). The next step involves an intramolecular cyclization with an activation energy of 6.6 kcal/mol to create a non-classical cation intermediate **5**, stabilized by charge delocalization between the two potential electrophilic sites ***a*** and ***b***. At this step, the reaction can proceed through two different mechanisms: the nucleophilic attack of the indole (**2**) at benzylic site ***a*** (path a in Scheme 2) leads to the major product (**3**), while an attack on site ***b*** (path b in Scheme 2) leads to the minor isomer **3'**. The former nucleophilic attack is, contradictorily, more facile although by only 1.1 kcal/mol with respect to **TS$_{5\text{-}7}$**.[20] These results agree with the outcomes presented by Echavarren *et. al* in their recent study on the structure of 1,6-enyne Au(I) intermediates.[21] In fact, the access to the cyclopropyl gold(I) carbene **7** is favored both kinetically and thermodynamically, albeit marginally. In this case, however, the final protodeauration step can explain the remarkable chemoselectivity of the studied reaction. As a matter of fact, although product **3'** is thermodynamically favored its protodeauration is a kinetic bottleneck, requiring an activation energy of 25.3 kcal/mol, whereas the major product **3** is accessed through a protodeauration transition state requiring only 9.1 kcal/mol. Non statistical effects have sometimes been suggested to play an important role in bifurcating paths with closely competing transition states.[22] In this case, however, neither transition states have ambimodal features nor the energy profile is such that a strongly exergonic step is immediately followed by low energy and competing transition states. We could therefore safely assume that the reaction is operating under the transition state theory.

As a means to compare the efficiency and chemospecifity between the novel catalyst *PedroPhosAu* and the unsubstituted JohnPhosAu complex, we computed the same catalytic cycle in the presence of [*PedroPhosAu*$^+$] catalyst. Interestingly, in the case of *PedroPhos* (Scheme 2 - results reported in red) the energy of all intermediates is lowered by 4.0 ± 0.7 kcal/mol, suggesting a more efficient catalysis as well as stabilizing action towards the involved organo-gold species. With respect to its chemospecificity **3** *vs* **3'** an even greater energy difference between the two competing protodeauration transition states **TS$_{6\text{-}3}$** and **TS$_{7\text{-}3'}$** (16.1 kcal/mol for JohnPhosAu *vs.* 17.3 kcal/mol for *PedroPhos*Au) is observed, thus strongly suggesting that the final protodeauration step, as the key to account for the overall chemoselectivity. [23]

Finally, we tried to understand the increased chemoselectivity of the decorated catalysts compared to JohnPhosAu regardless of the electronic nature of the substituents on the distal phenyl ring. When analyzing the geometries of intermediate **5** for JohnPhosAuCl, *PedroPhosAuCl* and **Cat5** (devoid of substituents, EWG substituted and EDG substituted, respectively) we found that, in the two latter catalysts, the substrate rested at a similar conformation, while for JohnPhosAuCl it displayed a different pose (Scheme S5).This common orientation for the substituted catalysts strongly suggested an interaction between the CF3 or OMe substituents at distal phenyl ring of the catalyst and the aromatic pendant of the substrate. We therefore computed the NCIs of this non-classical cationic intermediate **5** for the three catalysts mentioned above. Our results showed that for both PedroPhosAuCl and **Cat5**, substitution at the terminal

phenyl ring enables additional non-covalent interactions between the substrate and the catalyst. These interactions stabilize the conformation of the substrate while their absence, as in the case of JohnPhos, makes the reacting complex more flexible, thus leading to a loss of selectivity.

For both gold intermediates **6** and **7**, the C-Au bond exhibits significant ionic character, as described by the Mulliken charges of -0.24 on C and +0.30 au on Au for **6**, and -0.37 on C and +0.39 au on Au for **7**. In parallel, the C-Au bond lengths do not differ significantly, measuring 2.14 and 2.01 Å for **6** and **7**, respectively. Moreover, the excellent control in stereoselectivity observed experimentally on compound *exo*-**3** can be explained by the thermodynamic instability of the intermediate that would lead to the *endo* product **3"** (see Supporting Information, Scheme S1).

To better quantify the accelerating effect of the newly proposed [*PedroPhos*Au$^+$] (**Cat1**), a comparative kinetic study involving **Cat1**, **JP** and **Cat5** was carried out with **1a** as the model substrate (Figure 2, see also Supporting Information for a comprehensive discussion). Initial reaction rates were conveniently determined by ^{1}H-NMR analysis. The data fitting revealed that *PedroPhos*AuCl outperforms the other catalysts (slope, s = 9.48 x 10^{-5}) also in this case. The electron rich arene containing catalysts **JP** (s = 2.96 x 10^{-5}) and **Cat5** (s = 2.57 x 10^{-5}) showed a close kinetic behavior and a $\Delta_{rate}/\Delta_{conc.}$ ca. 3.5 times lower than that **Cat1**.

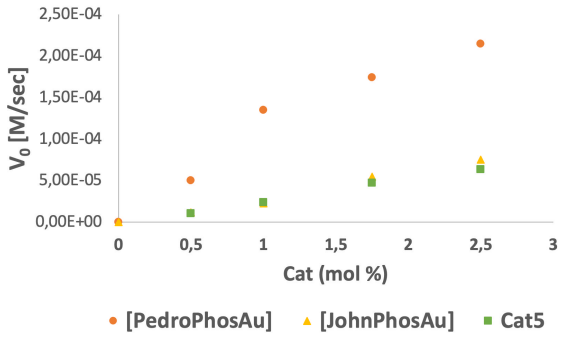

Figure 2. Plot of initial rate (V_0) *vs* catalyst loading (mol%). V_0 = molarity of **3a** produced per second.

During kinetic data elaboration, we noticed that the very initial catalytic cycles were elusive. For each experiment at t_1 = 30 s, [**3a**] was already 3 to 7 times higher than [**Cat**]. However, the subsequent data points exhibited a linear fit (refer to ESI for details). This evidence led us to consider a poisoning effect exerted by the initially formed reaction product on the catalytically active cationic complex. To explore this possibility, we conduced dedicated computations with [JohnPhosAu$^+$] as the model catalyst to support this hypothesis. Specifically, we calculated the thermodynamic difference between the final complex (JohnPhosAu + **3** or **3'**) and the precomplex constituted by JohnPhosAu + **1** and + **2**. In both cases, the final complex proved to be significantly more stable (34.3 kcal/mol (**3**) and 21.7 kcal/mol (**3'**)) than the precomplex, explaining the slowdown in the reaction as the concentration of **3a**/**3a'** increases. This theoretical prediction aligns remarkably well with the described behavior and contributes to a better understanding of the experimental kinetic studies presented in Figure S2.

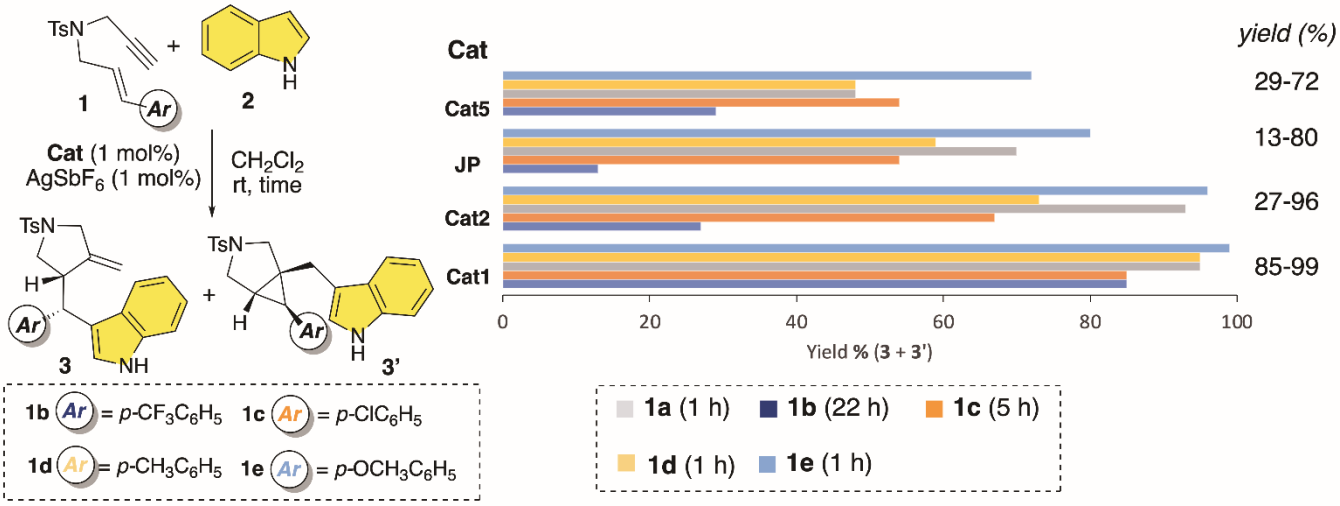

Scheme 3. Monitoring the catalytic performance of **Cat1**,**2**, **JP** and **Cat5** across a range of 1,6-enynes **1b-e**. All reactions were carried out under nitrogen atmosphere with dry solvents (**1**: 0.2 mmol, **1**/**2**: 1/1.2). Isolated yields after flash chromatography are reported as an average of three runs. Reactions with complex JP were carried out under silver-free conditions. JP: [JohnPhosAu(ACN)]SbF_6.

The accelerating effect imprinted by fluorinated biphenyls was further evaluated by subjecting a range of electronically diversified cinnamyl enynes **1b-e** to the cascade ring-closing process (Scheme 3). Several interesting trends can be extrapolated from these experiments: i) with exception of *p*Me-cinnamyl substrate **1d**, which exhibited a peculiar reactivity profile likely related to steric factors,[24] the highest conversions were recorded when the stronger EDG group -OMe was accommodated on the phenyl ring (**1e**). This evidence suggests that the nucleophilic condensation of the styryl C=C bond on the gold activated C-C triple bond strongly influences the overall reaction rate; ii) **Cat1** (containing *PedroPhos* ligand) demonstrated superior performance among all the gold complexes and across all investigated substrates. As a matter of fact, under comparative reaction times (1-22 h), the highest isolated yields were achieved (85-99%). Notably, **Cat1** was capable of catalyzing the cyclization of the poorly nucleophilic CF_3-containing cinnamyl substrate **1b** (85% yield, 22 h), while the classic silver-free JohnPhos-based gold complex delivered **3b** with only a 13% isolated yield.

Furthermore, to bolster the evidence supporting the superiority of the *PedroPhosAuCl* complex in the electrophilic activation of alkynes, the catalytic performances of **Cat1-5** were also tested at a 1 mol% loading in the hydroindolynation of alkyne **8** upon *in situ* activation with $AgSbF_6$.[25] The collected chemical outcomes have been summarized in Scheme 4. Remarkably, even in this intramolecular activation of terminal alkynes, *PedroPhos*AuCl/$AgSbF_6$ **Cat 1** outperformed the other tested gold complexes, providing the tricyclic fused indole **9** in 84% isolated yield after 1 h reaction time (TOF: 84 h^{-1}, TON = 84). In particular, **Cat 1** exhibited superior catalytic performance with respect to JohnPhosAuCl/$AgSbF_6$ (20% yield after 1 h), fluorinated **Cat 3** (yield = 60%), the EDG-containing catalyst **Cat 5** and the adamantyl complexes **Cat 2**/**4** (yields up to 54%). In all cases, complete regioselectivity toward a *7-exo*-ring-closing process was confirmed.

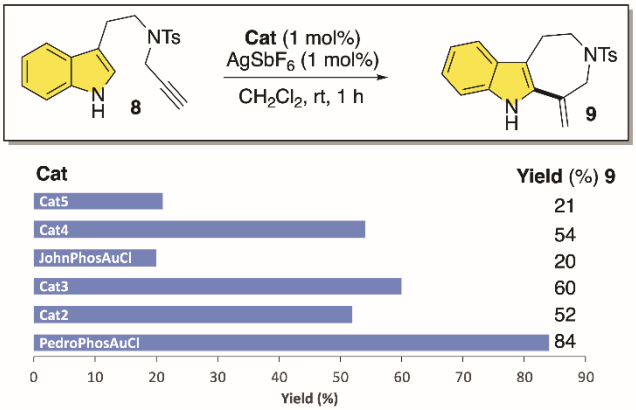

Scheme 4. Intramolecular hydroindolynation of alkynes. Comparative analysis of the catalytic performance of **Cat1-5** and JohnPhosAuCl. Isolated yield after flash chromatography as an average of three runs

In conclusion, our study details the synthesis and comprehensive characterization, both in solution and solid state, of a new family of phosphine ligands and their corresponding gold complexes. These complexes exhibit enhanced electrophilic activations towards alkyne modifications compared to existing state-of-the-art catalysts. The key innovation involves introducing electron-withdrawing substituents, such as CF_3, at the outer phenyl ring of JohnPhos-like ligands. This modification results in a remarkable balance between higher stabilization of the corresponding organogold intermediate (leading to increased turnover numbers, TON) and improved electrophilicity of the metal center (resulting in higher turnover frequencies, TOF). This synergistic effect was confirmed through both experimental and computational investigations involving a series of cationic gold complexes. These complexes were evaluated in the context of model transformations, specifically the hydroarylation of 1,6-enynes and the hydroindolynation of alkynes. The outcomes of this study pave the way for the development of highly efficient and selective gold-catalyzed transformations. The balance achieved between stability and reactivity in these new gold complexes holds promise for their application in a broader range of transformations and underscores the potential impact of electron-withdrawing substituents in the design of effective gold catalysts.

ASSOCIATED CONTENT

AUTHOR INFORMATION

Corresponding Author

* MM: magda.monari@unibo.it
* CSL: csilval@uvigo.gal
*MB: marco.bandini@unibo.it

AUTHOR CONTRIBUTIONS

The manuscript was written through contributions of all authors. All authors have given approval to the final version of the manuscript.

SUPPORTING INFORMATION

The Supporting Information is available free of charge on the ACS Publications website.
Synthesis, characterization of new ligands and gold complexes. Mechanistic investigation (file type: PDF)
Computational studies (file type: PDF)
Crystallographic data (file type: cif)
All the relevant structures (minima and TS) of the computational study are uploaded in the ioChem-BD repository(https://www.iochem-bd.org/) hosted at the Barcelona Supercomputing Center (https://www.bsc.es/), where carte-sian coordinates, energies and frequencies are made publicly available with the following doi: https://doi.org/10.19061/iochem-bd-6-329.

ACKNOWLEDGMENT

We are grateful to the University of Bologna for financial support. MB also thanks Consorzio CINMPIS. CSL thanks CESGA for allocation of HPC resources and MICINN for financial support (PID2020-115789GB-C22) and SK the Xunta de Galicia for funding through the fellowship “Ayudas de apoyo a la etapa de formación posdoctoral (ED481B-2023-044)”.

ABBREVIATIONS

Ad: adamantyl; dppf: 1,1′-bis(diphenylphosphino)ferrocene; EDG, electron donating group; EWG, electron withdrawing group; DMS: dimethylsulphide; JP: JohnPhos: (2-biphenyl)di-tert-butylphosphine; PedroPhos: (3',5'-bis(trifluoromethyl)-[1,1'-biphenyl]-2-yl)di-tert-butylphosphine.

REFERENCES

(1) For a collection of recent review articles on homogenous gold catalysis, see: a) Hashmi, A. S. K. Dual gold catalysis, *Acc. Chem. Res.*, **2014**, *47*, 864-876; b) Fürstner, A. From understanding to prediction: gold- and platinum-based π-acid catalysis for target oriented synthesis, *Acc. Chem. Res.*, **2014**, *47*, 925- 938; c) Obradors, C.; Echavarren, A. M. Intriguing mechanistic labyrinths in gold(I) catalysis, *Chem. Commun.*, **2014**, *50*, 16-28; d) Wang, Y.; Muratore, M.E.; Echavarren, A.M. Gold carbene or carbenoid: is there a difference? *Chem. –Eur. J.*, **2015**, *21*, 7332-7339; e) Joost, M.; Amgoune, A.; Bourissou, D. Reactivity of gold complexes towards elementary organometallic reactions, *Angew. Chem., Int. Ed.*, 2015, 54, 15022-15045; f) Hendrich, C.M.; Sekine, K.; Koshikawa, T.; Tanaka, K.; Hashmi, A.S.K. Homogeneous and heterogeneous gold catalysis for materials science, *Chem. Rev.* **2021**, *121*, 9113-9163; g) Collado, A.; Nelson, D.J.; Nolan, S.P. Optimizing catalyst and reaction conditions in gold(I) catalysis-ligand development, *Chem. Rev.* **2021**, *121*, 8559-8612; h) Campeau, D.; León Rayo, D.F.; Mansour, A.; Muratov, K.; Gagosz, F. *Chem. Rev.* **2021**, *121*, 8756-8867; i) Scattolin, T.; Tonon, G.; Botter, E.; Guillet, S.G.; Tzouras, N.V.; Nolan, S.P. Gold(I)-*N*-heterocyclic carbene synthons in organometallics synthesis, *Chem. Eur. J.* **2023**, *29*, e202301961.

(2) a) Klahn, P.; Kirsch, S. F. Electronic fine-tuning of carbene ligands and its impact on gold catalysis. *ChemCatChem* **2011**, *3*, 649-652; b) Wang, W.; Hammond, G.B.; Xu, B. Ligand effects and ligand design in homogeneous gold(I) catalysis, *J. Am. Chem. Soc.* **2012**, *134*, 5697-5705; c) Wang, Y.; Wang, Z., li, Y.; Wu, G.; Cao, Z.; Zhang, L. *Nat. Commun.* **2014**, *5*, 10.1038/ncomms4470; d) Cheng, X.; Zhang, L. Designed bifunctional ligands in cooperative homogenous gold catalysis, *CCS Chem* **2020**, *2*, 1989-2002; e) Collado, A.; Nelson, D.J.; Nolan, S.P. *Chem. Rev.* **2021**, *121*, 8559-8612; f) Martinze, T.; Vanitcha, A.; Troufflard, C.; Vanthuyne, N.; Forté, J.; Gontard, G.; Lemière, G.; Mourìes-Mansuy, V.; Fensterbank, L. Indolizy carbene ligand. Evaluation of electronic properties and applications in asymmetric gold(I) catalysis. *Angew. Chem. Int. Ed.* **2021**, *60*, 19879; g) Teixeira, P.; Bastin, S.; César, V. Fused polycyclic NHC ligands in gold catalysis: recent advances, *Isr. J. Chem.* **2022**, e202200051. See also: Muratov, K.; Gagosz, F. Confinemnt-indiced selectivities in gold (I) catalysis-the benefit of using bulky tri-(*ortho*-biaryl)phosphine ligands. *Angew. Chem. Int. Ed.* **2022**, *61*, e202203452

(3) Sustainable catalysis: a) Kumar, A.; Patil, N.T., Ligand-enabled sustainable gold catalysis, *ACS Sust. Chem. Eng.* **2022**, *10*, 6990-6918; Redox chemistry: b) Huang, B.; Hu, M.; Toste, F. D. Homogeneous gold redox chemistry: organometallics, catalysis, and beyond. *Trends Chem*. **2020**, *2*, 707-720; c) Font, P.; Ribas, X. Fundamental basis for implementing oxidant-free Au(I)/Au(III) catalysis, *Eur. J. Inorg. Chem.* **2021**, 2556-2569; asymmetric catalysis: d) Cera, G.; Bandini, M. Enantioselective gold(I) catalysis with chiral monodentate ligands, *Isr. J. Chem.* **2013**, *53*, 848-855; e) Wang, Y.-M.; Lackner, A.D.; Toste, F.D. Development of catalysts and ligands for enantioselective gold catalysis, *Acc. Chem. Res.* **2014**, *47*, 889–901; f) Zuccarello, G.; Escofet, I.; Caniparoli, U.; Echavarren, A. E., New-generation ligand design for the gold-catalyzed asymmetric activation of alkynes, *ChemPlusChem*, **2021**, *86*, 1283-1296; g) Mishra, S.; Patil, N.T. Chiral ligands for Au(I), Au(III), and Au(I)/Au(III) redox catalysis, *Isr. J. Chem.* **2023**, *63*, e2022000039; h) Melot, R.; Michelet, V. Coinage metal-catalyzed asymmetric reactions of *ortho*-alkynylaryl and heteroaryl aldehydes and ketones, *Molecules* **2022**, *27*, 6970; i) Ambegave, S.B.; More, T.R.; Patil, N.T. Gold-based enantioselective bimetallic catalysts, *Chem. Commun.* **2023**, *59*, 8007-8016; total synthesis: l) De, S.; Dan A.K.; Sahu, R.; Parida, S.; Das, D. Total synthesis of natural products using gold catalysis**,** *Chem. Asian J.* **2022**, e202200896; photocatalysis: m) Witzel, S.; Hashmi, A.S.K.; Xie, J. Light in gold catalysis, *Chem. Rev.* **2021**, *121*, 8868-8925.

(4) For some representative examples see: a) Franchino, A.; Martí, À.; Nejrotti, S.; Echavarren, A. M. Silver-free Au(I) catalysis Enabled by Bifunctional urea- and squaramide-Phosphine Ligands via H-Bonding, *Chem. Eur. J.* **2021**, *27*, 11989-11996; b) Franchino, À.; Martí, A.; Echavarren, A.M. H-bonded counterion-directed enantioselective Au(I) catalysis, *J. Am. Chem. Soc.* **2022**, *144*, 3497-2509.

(5) a) Anderson, K. W., Tundel, R. E., Ikawa, T., Altman, R. A., Buchwald, S. L. Monodentate phosphines provide highly active catalysts for Pd-catalyzed C-N bond-forming reactions of heteroaromatic halides/amines and (H)N-heterocycles. *Angew. Chem. Int. Ed.* **2006**, *45*, 6523-6527; b) Billingsley, K., Buchwald, S. L. Highly efficient monophosphine-based catalyst for the palladium-catalyzed Suzuki Miyaura reaction of heteroaryl halides and heteroaryl boronic acids and esters, *J. Am. Chem. Soc.* **2007**, *129*, 3358-3366; c) Fors, B. P., Watson, D. A., Biscoe, M. R., Buchwald, S. L. A highly active catalyst for Pd-catalyzed amination reactions: cross-coupling reactions using aryl mesylates and the highly selective monoarylation of primary amines using aryl chlorides, *J. Am. Chem. Soc.* **2008**, *130*, 13552-13554

(6) Zuccarello, G.; Zanini, M.; Echavarren, A.M. Buchwald-type ligands on gold(I) catalysis, *Isr. J. Chem.* **2020,** *60*, 360-372.

(7) a) Herrero-Gómez, E.; Nieto-Oberhuber, C.; Lopez, S.; Benet-Buchholz, Echavarren, A. E. *Angew. Chem. Int. Ed.* **2006**, *45*, 5455-5459; b) Pérez-Galán, P.; Delpont, N.; Herrero-Gómez, E.; Maseras, F.; Echavarren, A.M. Metal–arene interactions in dialkylbiarylphosphane complexes of copper, silver, and gold, *Chem. Eur. J.* **2010**, *16*, 5324-5332.

(8) For some representative examples see: a) Nicholls, L.D.M.; Marx, M.; Hartung, T.; González-Fernández, E.; Golz, C.; Alcarazo, M. TADDOL-derived cationic phosphonites: toward an effective enantioselective synthesis of [6]helicenes via Au-catalyzed alkyne hydroarylation, *ACS Catal.* **2018**, *8*, 6079-6085; b) Deck, E.; Wagner, H.E.; Paradies, J.; Breher, F. Redox-responsive phosphonite gold complexes in hydroamination catalysis, *Chem. Commun.* **2019**, *55*, 5323-5326.

(9) a) Zuccarello, G.; Mayans, J. G.; Escofet, I.; Scharnagel, D.; Kirillova, M. S.; Pérez-Jimeno, A. H.; Calleja, P.; Boothe, J. R.; Echavarren, A. M. Enantioselective folding of enynes by gold(I) catalysts with a remote C_2-chiral element. *J. Am. Chem. Soc.* **2019**, *141*, 11858−11863; b) Chen g, X.; Zhang, L. Chiral bifunctional phosphine ligand enables gold-catalyzed asymmetric isomerization and cyclization of propargyl sulfonamide into chiral 3-pyrroline, *Org. Lett.* **2022**, *23*, 8194-8198; c) Caniparoli, U.; Escofet, I.; Echavarren, A.M. Planar chiral 1,3-disubstituted ferrocenyl phosphine gold(I) catalysts, *ACS Catal.* **2022**, *12*, 3317-3322; d) Zuccarello, G.; Nannini, L.J.; Arroyo-Bondía, A.; Fincias, N.; Arranz, I.; Pérez-Jimeno, A.H.; Peeters, M.; Martín-Torres, I.; Sadurní, A.; García-Vasquez, V.; Wang, Y.; Kirilova, M.S.; Monteisnos-Magraner, M.; Caniparoli, U.; Núñez, G.D.; Maseras, F.; Besora, M.; Escofet, I.; Echavarren, A.M. Enantioselective catalysis with pyrrolidinyl gold(I) complexes: DFT and NEST analysis of the chiral binding pockets, *JACS Au* **2023**, *3*, 1742-1754.

(10) a) Pedrazzani, R.; Pintus, A.; De Ventura, R.; Marchini, M., Ceroni, P.; López, C.S.; Monari, M.; Bandini, M. Boosting gold(I) catalysis via weak interactions: new fine-tunable ImPy ligands, *ACS Org. Inorg. Au* **2022**, *2*, 229-235; b) Pedrazzani, R.; Pinosa, E.; Bertuzzi, G.; Monari, M.; Lauzon, S.; Ollevier, T.; Bandini, M. Convenient synthesis of tricyclic N(1)-C(2)-fused oxazino-indolones via [Au(I)] catalyzed hydrocarboxylation of allenes, *Chem. Commun.* **2022**, *58*, 8698-8701.

(11) Tappe, F.M.J.; Trepohl, V.T.; Oestreich, M. Transition-metal-catalyzed C-P cross-coupling reactions, *Synthesis*, **2010**, 3037-3062; b) Wauters, I.; Debrower, W.; Stevens, C.V. Preparation of phosphines through C-P bond formation, *Beistein J. Org. Chem.* **2014**, *10*, 1064-1096.

(12) For representative gold catalyzed addition of indoles to 1,6-enynes see: a) Amijs, C.H.M., Ferrer, C., Echavarren, A.E. Gold(I)-catalysed arylation of 1,6-enynes: different site reactivity of cyclopropyl gold carbenes *Chem. Commun.* **2006**, 698-700; b) Amijs, C.H., Lopez-Carrillo, V.; Raducan, M.; Pérez-Galan, Ferre, C.; Echavarren, A.M., Gold-catalyzed intermolecular addition of carbon nucleophiles to 1,5- and 1,6-enynes, *J. Org. Chem.* **2008**, *73*, 7721-7730; c) Seo, H.; Roberts, B.P.; Abboud, K.A.; Merz Jr, K.M.; Hong, S., Novel acyclic diaminocarbene ligands with increased steric demand and their application in gold catalysis, *Org. Lett.* 2010, 12, 4860-4863; d) Leseurre, L.; Chao, C.-M.; Seki, T.; Genin, E.; Toullec, P.Y.; Genêt, J.-P.; Michelet, V. Synthesis of functionalized carbo- and heterocycles via gold-catalyzed cycloisomerization reaction of enynes. *Tetrahedron*, **2009**, *65*, 1911-1918; e) de Frémont, P.; Clavier, H.; Rosa, V.; Avilés, T.; Braunstein, P. Synthesis, characterization, and reactivity of cationic gold(I) α-diimine complexes, *Organometallics,* **2011**, *30*, 2241-2251; f) Teci, M.; Hueber, D.; Pale, P.; Toupet, L.; Blanc, A.; Brenner, E.; Matt, D. Metal confinement through *N*-(9-alkyl)fluorenyl-substituted N-heterocyclic carbenes and its consequences in gold-catalyzed reactions involving enynes, Chem. *Eur. J.* **2017**, *23*, 7809-7818; g) Pradal, A.; Chao, C.-M.; Vitale, M. R.; Toullec, P. Y.; Michelet, V. Asymmetric Au-catalyzed domino cyclization/nucleophile addition reactions of enynes in the presence of water, methanol and electron-rich aromatic derivatives, *Tetrahedron*, **2011**, *67*, 4371-4377; h) Carreras, J.; Pereira, A.; Zanini, M.; Echavarren, A.M. Variations on the theme of JohnPhos gold(I) catalysts: arsine and carbene complexes with similar architectures, *Organometallics*, **2018**, *37*, 3588-3597; i) Ruch, A.A.; Ellison, M.C.; Nguyen, J.K.; Kong, F.; Handa, S.; Nesterov, V.N.; Slaughter, L.M. Highly sterically encumbered gold acyclic diaminocarbene complexes: overriding electronic control in regiodivergent gold catalysis, *Organometallics*, **2021**, *40*, 1416-1433; j) V. Michelet, Gold-catalyzed reactions towards diversity: from simple substrates to functionalized carbo- and heterocycles, *Chem. Rec.* **2021**, *21*, 3884-3896;

(13) J.-D. Chai, M. Head-Gordon, Long-range corrected hybrid density functionals with damped atom–atom dispersion corrections, *Phys. Chem. Chem. Phys.* **2008**, *10,* 6615-6620

(14) . D. Andrae, U. Häußermann, M. Dolg, H. Stoll, H. Preuß. Energy-adjusted ab initio pseudopotentials for the second and third row transitions elements, *Theor. Chim. Acta* **1990**, *77*, 123-144.

(15) All the geometry optimizations were carried out using the Gaussian 16 code, Revision C.01, Frisch, M. J.; Trucks, G. W.; Schlegel, H. B.; Scuseria, G. E.; Robb, M. A.; Cheeseman, J. R.; Scalmani, G.; Barone, V.; Petersson, G. A.; Nakatsuji, H.; Li, X.; Caricato, M.; Marenich, A. V.; Bloino, J.; Janesko, B. G.; Gomperts, R.; Mennucci, B.; Hratchian, H. P.; Ortiz, J. V.; Izmaylov, A. F.; Sonnenberg, J. L.; Williams-Young, D.; Ding, F.; Lipparini, F.; Egidi, F.; Goings, J.; Peng, B.; Petrone, A.; Henderson, T.; Ranasinghe, D.; Zakrzewski, V. G.; Gao, J.; Rega, N.; Zheng, G.; Liang, W.; Hada, M.; Ehara, M.; Toyota, K.; Fukuda, R.; Hasegawa, J.; Ishida, M.; Nakajima, T.; Honda, Y.; Kitao, O.; Nakai, H.; Vreven, T.; Throssell, K.; Montgomery, J. A., Jr.; Peralta, J. E.; Ogliaro, F.; Bearpark, M. J.; Heyd, J. J.; Brothers, E. N.; Kudin, K. N.; Staroverov, V. N.; Keith, T. A.; Kobayashi, R.; Normand, J.; Raghavachari, K.; Rendell, A. P.; Burant, J. C.; Iyengar, S. S.; Tomasi, J.; Cossi, M.; Millam, J. M.; Klene, M.; Adamo, C.; Cammi, R.; Ochterski, J. W.; Martin, R. L.; Morokuma, K.; Farkas, O.; Foresman, J. B.; Fox, D. J. Gaussian, Inc., Wallingford CT, **2016**.

(16) Praveen, C.; Szafert, S. Homogenous gold catalysis for regioselective carbocyclization of alkynyl precursors, *ChemPlusChem*, **2023**, *88*, e202300202.

(17) Calculated TOF values are referred to initial reaction rates: **Cat1**: 1.5 min, JohnPhosAuCl: 3 min and **Cat5**: (1. 5 min).

(18) a) Becke, A.D. Density-functional thermochemistry. III. The role of exact exchange, *J.Chem.Phys*. **1993**, *98*, 5648-5652; b) Stephens, P.J.; Devlin, F.J.; Chabalowski, C.F.; Frisch, M.J. Ab Initio calculation of vibrational absorption and circular-dichroism spectra using density-functional force-fields, *J. Phys. Chem.* **1994**, *98,* 11623-11627

(19) a) Faza, O.N.; Rodríguez, R.Á.; López, C.S. Performance of density functional theory on homogeneous gold catalysis. *Theor. Chem. Acc.* **2011**, *128*, 647–661 b) Faza, O.N., López, C.S. (2014). Computational Approaches to Homogeneous Gold Catalysis. In: Slaughter, L. (eds) Homogeneous Gold Catalysis. Topics in Current Chemistry, vol 357. Springer, Cham.

(20) Shough, A.M.; Doren, D.J.; Di Toro, D.M. Polyfunctional methodology for improved DFT thermochemical predictions. *J. Phys. Chem. A,* **2008**, *112*, 10624-10634

(21) Escofet, I.; Armengol-Relats, H.; Bruss, H.; Besora, M.; Echavarren A.M. On the structure of intermediates in enyne gold(I)-catalyzed cyclizations: formation of *trans*-fused bicyclo[5.1.0]octanes as a case study, *Chem. Eur. J.* **2020**, *26*, 15738-15745.

(22) a) Samanta, D.; Rana, A.; Schmittel, M. Nonstatistical Dynamics in the Thermal Garratt–Braverman/[1,5]-H Shift of One Ene–diallene: An Experimental and Computational Study, *J. Org. Chem*. **2014**, *79*, 8435-8439; b) Villar López, R.; Faza, O. N.; Silva López, C. Dynamic Effects Responsible for High Selectivity in a [3,3] Sigmatropic Rearrangement Featuring a Bispericyclic Transition State. *J. Org. Chem.* **2017**, *82*, 4758– 4765 c) Mandal, N.; Datta, A. Gold(I)-Catalyzed Intramolecular Diels–Alder Reaction: Evolution of Trappable Intermediates via Asynchronous Transition States, *J. Org. Chem*. **2018**, *83*, 11167-11177 d) Tantillo, D. Chapter One - Beyond transition state theory—Non-statistical dynamic effects for organic reactions, *Adv. Phys. Org. Chem.* **2021**, *55*, 1-16

(23) a) Amijs, C.H.M.; Ferrer, C.; Echavarren, A.M. Gold(I)-catalysed arylation of 1,6-enynes: different site reactivity of cyclopropyl gold carbenes. *Chem. Commun*. **2007**, *7*, 698-700 b) Stylianakis, I.; Nieto Faza, O.; Silva López, C.; Kolocouris, A.; The key role of protodeauration in the gold-catalyzed reaction of 1,3-diynes with pyrrole and indole to form complex heterocycles. *Org. Chem. Front.* **2020**, *7*, 997-1005 c) Cataffo, A.; Peña-López, M.; Pedrazzani, R.; Echavarren, A. M.; Chiral Auxiliary Approach for Gold(I)-Catalyzed Cyclizations. *Angew. Chem. Int. Ed.* **2023**, *62*, e202312874

(24) Although a conclusive explanation to rationalized the peculiar behavior **1d** is still elusive, we could speculate that combination of the higher steric impact of methyl group with respect to more structurally flexible OMe and the higher chemical reactivity displayed by **1e** over all other compounds could justify the observed trend of reactivity.

(25) a) Ferrer, C.; Echavarren, A. M. Gold-catalyzed intramolecular reaction of indoles with alkynes: facile formation of Eight-membered rings and an unexpected allenylation, *Angew. Chem. Int. Ed.* **2006**, *45*, 1105-1109; b) Ferrer, C.; Amijs, C. H. M.; Echavarren, A. M. Intra- and intermolecular reactions of indoles with alkynes catalyzed by gold, *Chem. Eur. J.* **2007**, *13*, 1358 1373; c) Zhu, P.-L.; Zhang, Z.; Tang, X.-Y.; Marek, I.; Shi, M. Gold- and silver-catalyzed intramolecular cyclization of indolylcyclopropenes for the divergent synthesis of azepinoindoles and spiroindoline piperidines, *ChemCatChem* **2015**, *7*, 595-600.

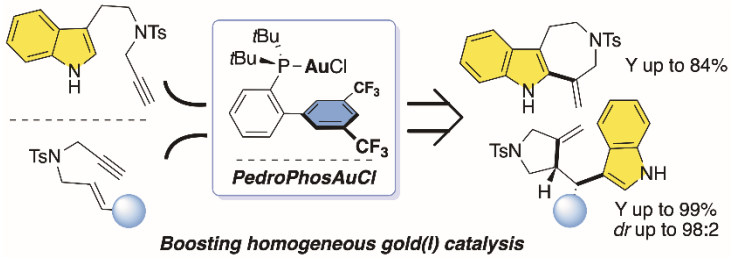

Boosting homogeneous gold(I) catalysis